Dynamic stall of a pitching and horizontally oscillating airfoil

G. Martinat, M. Braza, G. Harran, A. Sevrain

Institut de Mécanique des Fluides de Toulouse, Unité Mixte C.N.R.S.-I.N.P.T. 5502, Av. du Prof. Camille Soula, 31400 Toulouse, France

G. Tzabiras

Naval Architecture and Marine Engineering Department, National Technical University of Athens

Y. Hoarau

Intitut de Mécanique des Fluides et des Solides de Strasbourg

D. Favier

Laboratoire d'Aerodynamique et de Biomecanique du Mouvement de Marseille

Abstract. This paper provides a study of the dynamic stall of a pitching airfoil and of a pitching and horizontally oscillating airfoil at 10^5 Reynolds number by means of nbumerical simulation. 3 turbulence models are compared in both cases : URANS Spalart-Allmaras model, URANS $k-\varepsilon$ Chien model and URANS/OES model. Results are in accordance with experimental data but Spalart model seems to be too much viscous to provide good results and overpredict hysteresis cycle observed where URANS/OES seems to be viscousless. URANS $k-\varepsilon$ Chien model is providing the best results.

Keywords: dynamic stall, URANS/OES, pitching airfoil, incompressible flow.

1. Introduction

The prediction of the dynamic stall phenomenon at high Reynolds number is a crucial need in aeronautics and more specifically in rotorcraft dynamics. In this context, the forced unsteadiness (organised motion) interacts non-linearly with the fine-scale, random turbulence and produce a strong irreversibility effect that usually leads to hysteresis loops in the aerodynamic coefficients versus the angle of incidence. Under these conditions of strong non-equilibrium turbulence, standard modelling approaches are often insufficient to predict the dynamic stall at high Reynolds number. Under the above effects, the stall angle is found higher than the normal static stall one. The applications of these flows occur in turbomachinery and in helicopter rotorblades as well as in wind turbine airfoils. It is important to have a good prediction of the dynamic stall to ensure efficiency for the design. A comprehensive review of the dynamic stall phenomenon is described in [1] and [2].

In the present study, the motion of pithcing and then, the simultaneous motion of a pitching and horizontally oscillating NACA 0012 airfoil is analysed by means of CFD, using an appropriate turbulence modelling approach and comparison with experimental data.

2. Turbulence modeling : macrosimulation approaches for unsteady flows

The periodic nature of the flow past an oscillating airfoil allows the definition of phase averaged quantities. the flow is classically decomposed into a mean component, a periodic fluctuation and a random fluctuation [3] : $U_i = \overline{U_i} + \tilde{U}_i + \tilde{u_i}$. The phase averaged quantities is then $< U_i >= \overline{U_i} + \tilde{U}_i$ ([4]). Figure 1 shows the energy spectrum obtained on the experiment on a circular cylinder at high Reynolds number with LDV and PIV (Perrin and al, 2006) compared to the decomposition $U_i =< U_i > +\tilde{u_i}$. Due to a non linear interaction of chaotic with organised structure the slope of the fluctuation spectrum in the inertial part is different than the one of turbulence in equilibrium. As a consequence, when we model this spectrum we should consider that production is not equal to dissipation like in URANS equilibrium turbulence modelling, but instead we need to reconsider the turbulence time and length scales.

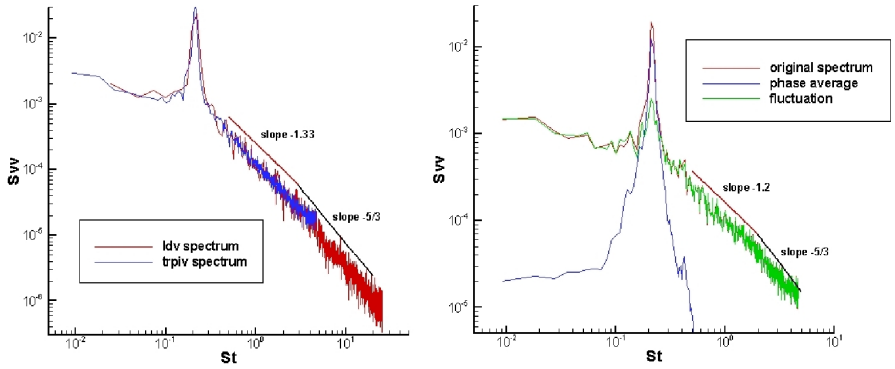

Figure 1. Velocity spectrum in a cylinder wake at Reynolds=140000. Experimental datas from PIV [5] and LDV [6]

In the context of advanced URANS methods, EMT2/IMFT has developped the Organised Eddy Simulation (O.E.S) approach ([7]). This consists in distinguishing the structures to be resolved from the one to be modeled on the basis of their physical nature, organised or chaotic and not on their size (this is the case in the LES approach).
The advantages of this approach are the robustness at high Reynolds number wall flows and the fact that the method is not intrinsically three-dimensional. From the second order moment closure DRSM [8] a modified two equation model has been derived, where the turbulent length scales have been modified in the sense of evaluation of the C_μ eddy diffusion coefficient and of the damping turbulence law towards the wall ([9] and [7]). In addition, a tensorial OES eddy-viscosity model has been derived to capture the non equilibrium turbulence ([10]) where the C_μ coefficient varies according to a directional criterion of stress-strain misalignment.

In this context, isotropic OES modeling is derived from $k-\epsilon$ Chien modeling ([11]) which is described by the following equation system :

$$\frac{Dk}{Dt} = \frac{\partial}{\partial y}[(\nu+\nu_t)\frac{\partial k}{\partial y}] + \nu_t(\frac{\partial \overline{U}}{\partial y})^2 - \epsilon - \frac{2\nu k}{y^2}$$

$$\begin{aligned} \frac{D\epsilon}{Dt} &= \frac{\partial}{\partial y}[(\nu + \frac{\nu_t}{\sigma})\frac{\partial \epsilon}{\partial y}] + C_1 \frac{\epsilon}{k}\nu_t(\frac{\partial \overline{U}}{\partial y})^2 - \frac{\epsilon}{k}[C_2 f_\epsilon + \frac{2\nu k e^{-C_4 \frac{U_* y}{\nu}}}{y^2}] \\ \nu_t &= C_\mu f_\mu(\frac{k^2}{\epsilon}) \end{aligned} \quad (1)$$

where $f_\epsilon = 1 - \frac{0.4}{1.8}e^{-(\frac{k^2}{6\nu\epsilon})^2}$ and $f_\mu = 1 - e^{-C_3 \frac{U_* y}{\nu}}$

Modification for OES are given by equation 2

$$\begin{aligned} f_\mu &= 1 - exp(-0.0002y^+ - 0.000065y^{+2}) \\ C_\mu &= 0.02 \end{aligned} \quad (2)$$

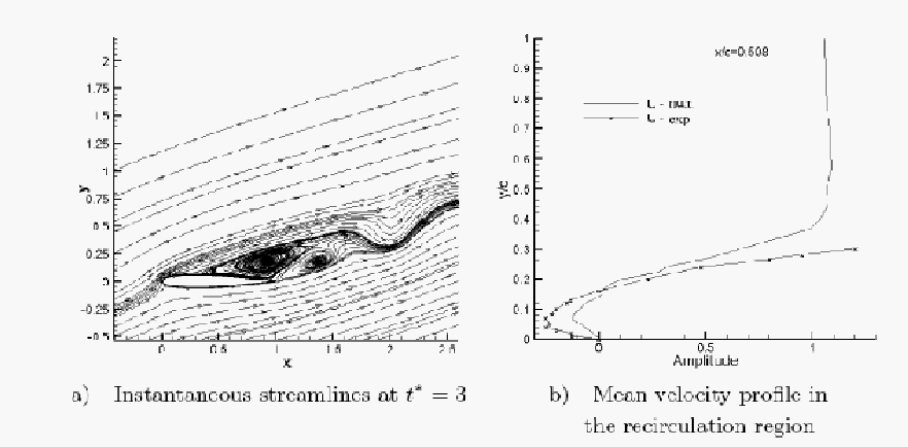

a) Instantaneous streamlines at $t^* = 3$ b) Mean velocity profile in the recirculation region

Figure 2. Instantaneous iso-vorticity lines at $t^* = 3$ using OES modelling and mean velocity profile in the recirculation region for a NACA0012 at 20^o of incidence and a Reynolds number of 10^5

This model was compared to experimental results provided by LABM laboratory on

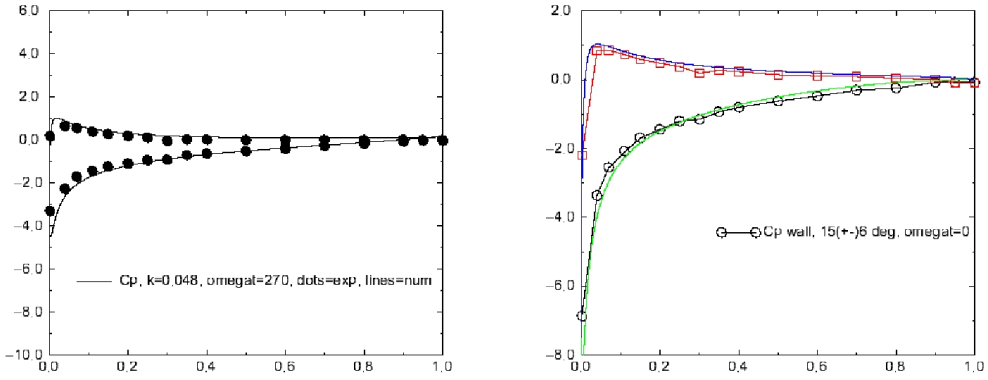

Figure 3. Comparison between OES and LABM experiment on a NACA0012 pitching airfoil, Reynolds number $Re = 10^6$, $\alpha = 15^{+}_{-}6^o$ and reduced frequency k=0.048

NACA0012 at 20^o of incidence for a Reynolds number of 10^5 and on a low frequency pitchiong airfoil (figure 3). Good results were obtained on that test case as seen on figure 2.

In the present studies, the isotropic version of the OES modeling has been used and the computations were performed using the NSMB solver (Navier Stokes Multi Block, developped by EPFL and KTH, [12]), a solver that is also used by Airbus France, in which we contributed by upgrading the unsteady turbulence modelling approaches. OES modeling has been compared to two URANS model : the Spalart-Allmaras one equation model ([13]) and the two equation $k - \epsilon$ Chien model.

3. Physical analysis of the dynamic stall around a pitching airfoil

The term dynamic stall usually refers to unsteady separation and stall phenomena on airfoils that are forced to execute time dependant motion. If the angle of attack oscillates around a mean value which is of the order of the static stall angle, large hysteresis cycles develop in the aerodynamic forces and moment. Indeed, during the upstroke motion, the effet of adversure pressure gradient is limited, driving to a dynamic stall angle which largely exceeds the static one whith aerodynamic that also greatly exceeds their static counterparts. During the downstroke part of the motion, the effect of adverse pressure gradient is reinforced, leading to a reattachment incidence angle which is lower than in the static case.

For this study, the airfoil performs a sinusoidal pitching motion around the quarter chord point. The mean pitch angle is $\alpha_0 = 12^o$ and the amplitude of pitch is $\Delta\alpha = 6^o$. The reduced frequency which is based on half chord length is $k = \frac{\omega c}{2U_\infty} = 0.188$.
The meshgrid used is C topology structured mesh, it has 256 cells in the I direction and 80 cells in the J direction, and is validated in hoarau and al, 2002. The solver uses third order upwind-roe space scheme and dual-time stepping with second order implicit backwards time-scheme. The time step varies along the computation by using constant CFL.

Figures 4 and 5 are respectively showing vorticity fields and pressure coefficient as a function of chord for 10 diffrents angle of attack. For 7.2^o to 12^o upstroke angle of attack, pressure coefficient shows a flow that remains attached to the profile . We can see either that pressure coeffcient is dedreasing on upper surface and increasing on the lower surface, leading to an increase on the lift coefficient. For 14.4^o, Pressure coefficent plot is showing the birth of a leading edge vortex which grows with the rise in incidence as shown on 16.8^o incidence upstroke vorticity field and pressure coefficient plot. For this angle of attack, we can notice that because of the growth of leading edge vortex, the pressure coeffient is homogeneous on the upper surface, so the pressure coeffcient is already decreasing near the leading edge where it is fastly increasing near the tailing edge. Because of this pressure distribution, we can observe a brutal rise on the drag coefficient which announce the dynamic stall that occurs when the leading edge vortex is shed at the end of the upstroke motion. That vortex shedding is immediately followed by the shed of a tailing edge vortex at the beginning of the downstroke motion. then, the flow remains detached until 6^o of incidence downstroke.

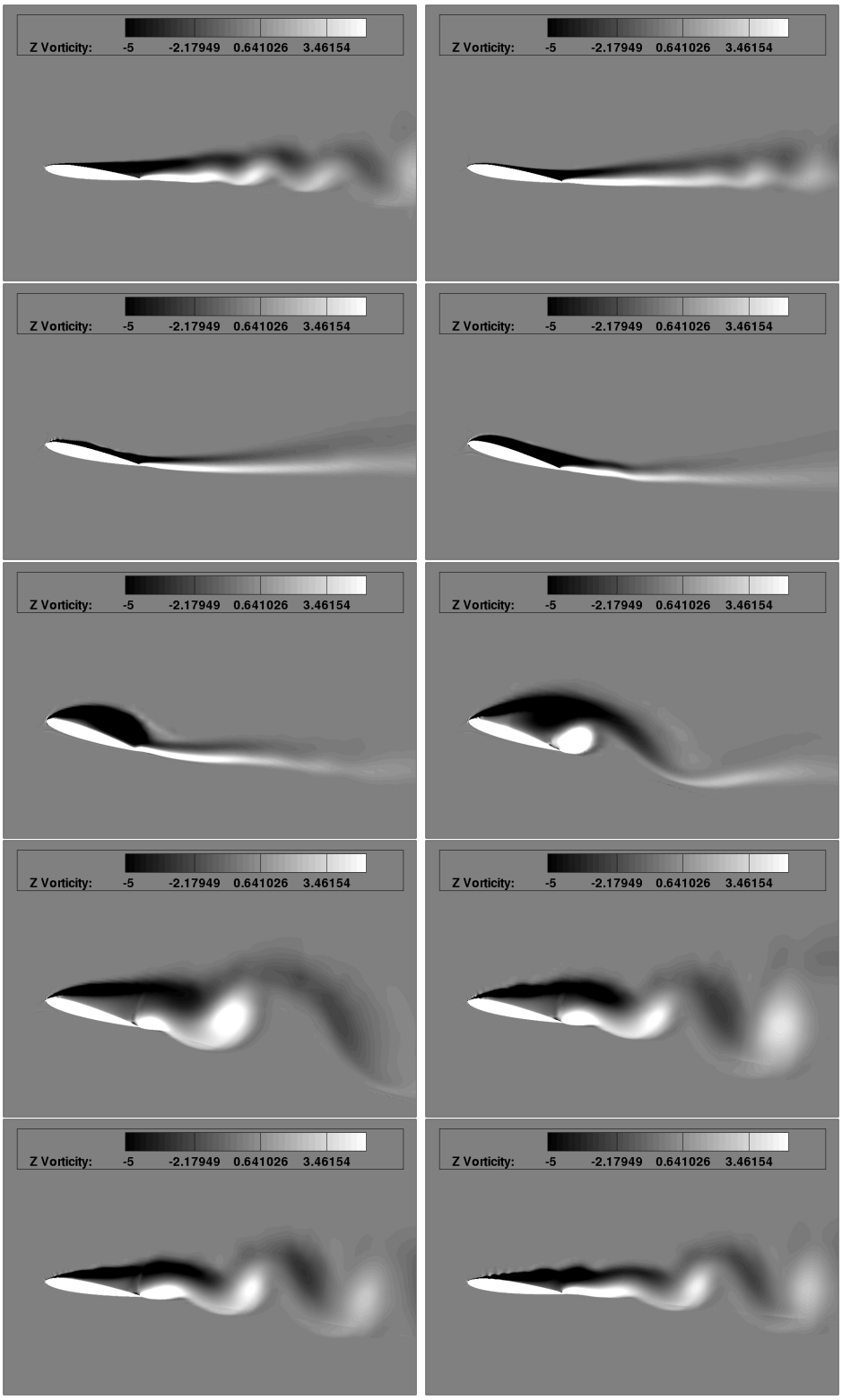

Figure 4. Isovorticity fields for 7.2^o, 9.6^o, 12^o, 14.4^o, 16.8^o *of incidence upstroke and* 16.8^o, 14.4^o, 12^o, 9.6^o *and* 7.2^o *of incidence downstroke*

Figure 6 is comparing results obtained on the pitching case with the three models performed. Spalart-Allmaras ([13]) modelling is giving hysteresis of too large area

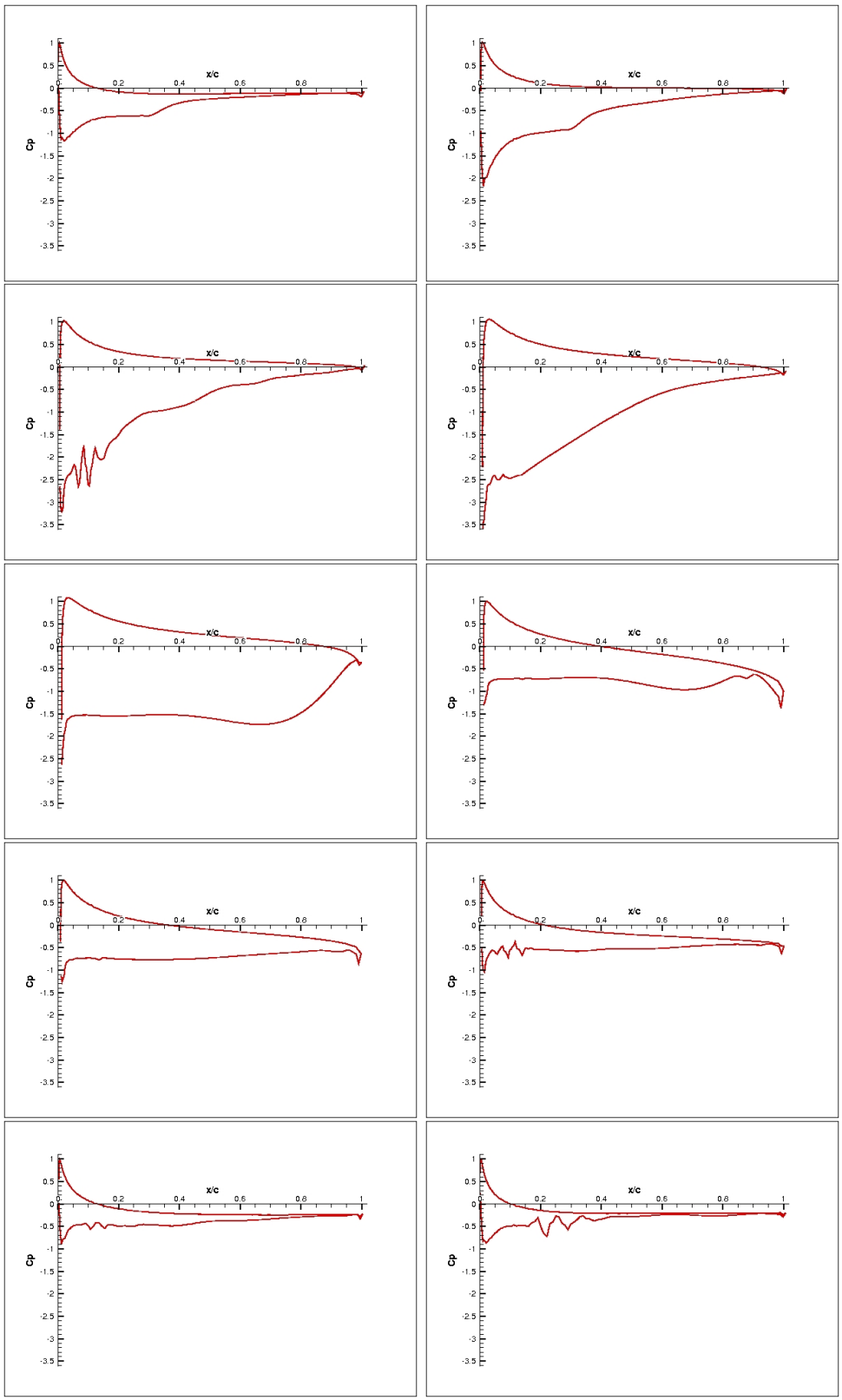

Figure 5. Pressure coefficient as a function of x/c for 7.2^o, 9.6^o, 12^o, 14.4^o, 16.8^o *of incidence upstroke and* 16.8^o, 14.4^o, 12^o, 9.6^o *and* 7.2^o *of incidence downstroke*

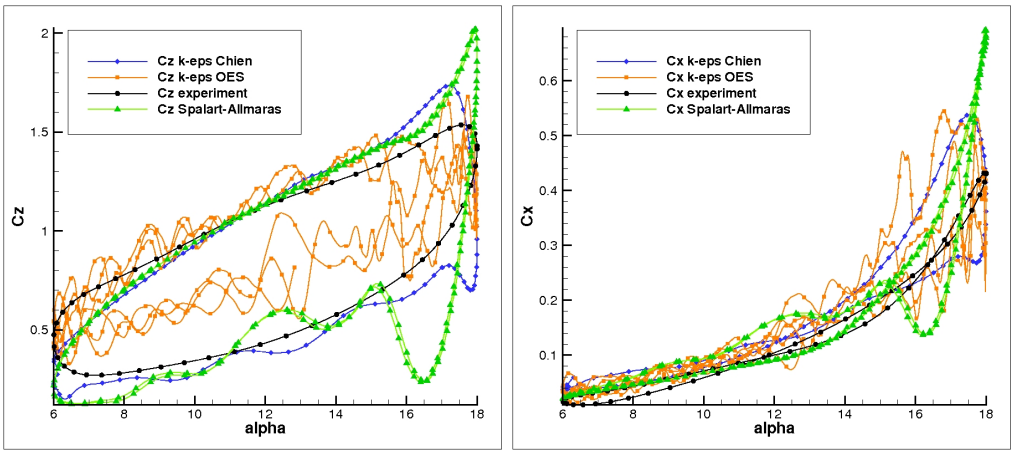

Figure 6. Hysteresis cycle obtained with the three different models on the pitching NACA0012 airfoil

and the lift and drag coefficient are overpredicted when dynamic stall occurs. $k-\varepsilon$ Chien model gives the most accurate results of the three models tested. the area of lift and drag coefficient hysteresis are still overpredicted as the values of lift and drag when stall occurs and the drag for every angle fo attack. $k-\varepsilon$ OES model gives results which are much noisy and more accurate than those which are provided by others model during the upstroke motion. However, the stall occurs too early and the lift coeffient is too high during the downstroke motion giving hysteresis cycle of too small area on the lift coeffcient. Those behaviors might be explained by the fact that the three turbulence model used are built on the concept of eddy viscosity. The prediction of eddy viscosity is then important to have have a good prediciton of leading and tailing edge vortices intensity. A too viscous model leads to the results observed with Spalart-Allmaras model, as the intensity of leading edge vortex is overpredicted, lift and drag coefficient are overpredicted at the end of the upstroke motion and dynamic stall occurs too late. A viscousless model leads to results observed with OES modelling, the dynamic stall occurs earlier and leading and tailing edge vortices intensity is under estimated.

4. Physical analysis of the dynamic stall around a pitching and horizontally oscillating airfoil

The airfoil performs here a sinusoidal pitching motion around the quarter chord point and sinusoidal and horizontal plunging motion. The mean pitch angle is $\alpha_0 = 12^o$ and the amplitude of pitch is $\Delta\alpha = 6^o$. Concerning the horizontally oscillating motion, the reduced frequency is the same as the pitching and the reduced amplitude is $\lambda = \frac{A\omega}{U_\infty} = 0.251$. The Reynolds number is 10^5 and the 2 mouvements are in phase. The experiment is presented [14].

During the the first part of the longitudinal oscillation, the perceived velocity is higher than the average velocity and tends to disadvantage stall as the rise in incidence during the pitch motion. the delerating phase of the moiton is supposed to support the detachment of the flow. ([14]).

Figure 7 shows the hysteresis cycle obtained with pitching and longitudinal os-

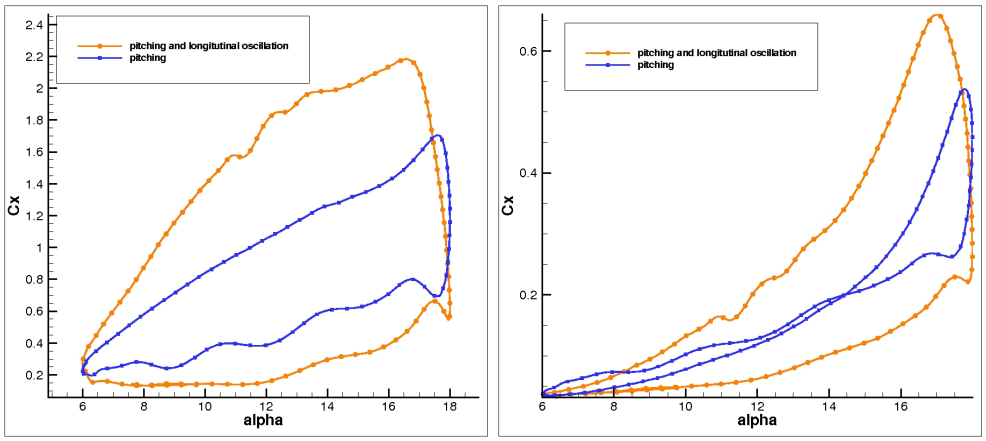

Figure 7. Comparison of the hysteresis cycle obtained with URANS $k-\varepsilon$ Chien modeling on the pitching NACA0012 airfoil and on the pitching and longitudinally oscillating NACA0012 airfoil by using mean infinite speed as reference speed for the lift coefficient calculation

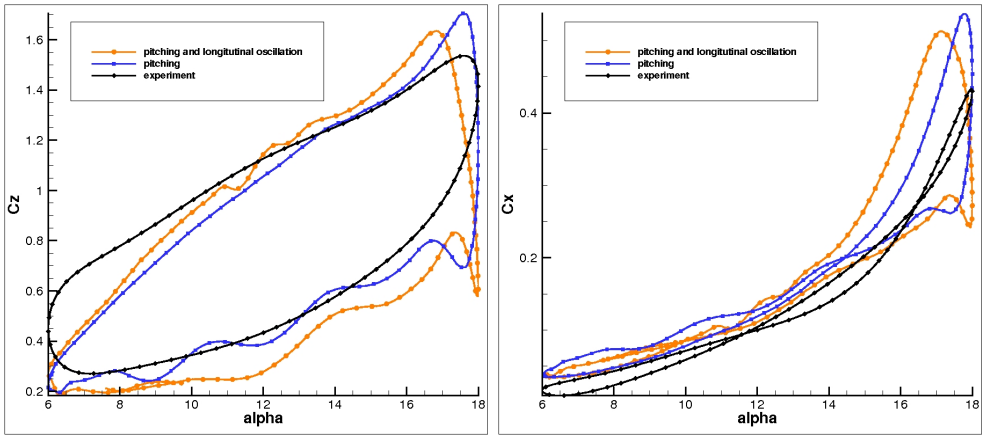

Figure 8. Comparison of the hysteresis cycle obtained with URANS $k-\varepsilon$ Chien modeling on the pitching NACA0012 airfoil and on the pitching and longitudinally oscillating NACA0012 airfoil to the experiment by using instantaneous infinite speed as reference speed for the lift coefficient calculation

cillating compared to the one obtained with pitching both with $k-\varepsilon$ Chien. We can observe that with the longitudinal oscillation, the hysteresis cycle area obtained is much larger than in the case without this oscillation. Figure 8 shows hysteresis cycles obtained on lift and drag coefficient for the pitching case and for the pitching and longitudinaly oscillating case where C_z is adimentionalised with the instantaneous infinite speed. On this figure, we observe that dynamic stall occurs earlier and area of hysteresis cycle are slightly bigger in the case with longitudinal oscillation. With this plot we can assume that the effect of longitudinal oscillation on the flow is almost linear. The bigger area of hysteresis cycle observed is due to a rise in speed during the upstroke part of the motion and a reduction of speed during the downstroke part.

5. Conclusion and prospects

In this study, the behavior of three different modelling is shown on the flow around a pitching airfoil and compared to experimental results. $k-\varepsilon$ provided the best results comparing with Spalart-Allmaras and $k-\varepsilon$ OES. Then, results on pitching airfoil are compared to the one obtained with a pitching and longitudinally oscillating airfoil. The small effect on the flow of longitudinal oscillation of the amplitude studied has been lightened.
Three dimensional study will be carried out in a near future as URANS/OES anisotropic modelling.

References

[1] W. J. McCroskey. Unsteady airfoils. *Annual Review of Fluid Mechanics*, 14, 1982.

[2] W. J. McCroskey. The phenomenon of dynamic stall. NASA report : NASA/TM-81264, 1981.

[3] W.C. Reynolds and A.K.M.F. Hussain. The mechanics of an organized wave in turbulent shear flow. part 3. theoretical models and comparison with experiments. *Journal of Fluid Mechanics*, 54, 1972.

[4] B. Cantwell and D. Coles. An experimental study of entrainment and transport in the turbulent near wake of a circular cylinder. *Journal of Fluid Mechanics*, 136:321–374, November 1983.

[5] R. Perrin, E. Cid, S. Cazin, A. Sevrain, M. Braza, F. Moradei, and G. Harran. Phase-averaged measurements of the turbulence properties in the near wake of a circular cylinder at high Reynolds number by 2C-PIV and 3C-PIV. *Experiments in Fluids*, 42:93–109, January 2007.

[6] H.Djeridi, M. Braza, R. Perrin, G. Harran, E. Cid, and S. Cazin. Near-wake turbulence properties around a curcular cylinder at high reynolds number. *Flow, Turbulence and Combustion*, 71:19–34, 2003.

[7] M. Braza, R. Perrin, and Y. Hoarau. Turbulence properties in the cylinder wake at high Reynolds numbers. *Journal of Fluids and Structures*, 22:757–771, August 2006.

[8] B.E. Launder, G.J. Reece, and W. Rodi. Progress in the development of a Reynolds-stress turbulence closure. *Journal of Fluid Mechanics*, 68:537–566, April 1975.

[9] G. Jin and M. Braza. A two equation turbulence model for unsteady separated flows around airfoils. *AIAA journal*, 32:2316–2320, 1994.

[10] R. Bourguet, M. Braza, R. Perrin, and G. Harran. Anisotropic eddy-viscosity concept for strongly detached unsteady flows. *AIAA journal*, 45:1145–1149, 2007.

[11] K. Chien. Prediction of channel and boundary-layer flows with a low reynolds number turbulence model. *AIAA journal*, 20:33–38, 1982.

[12] J. Vos, E. Chaput, B. Arlinger, A. Rizzi, and A. Corjon. Recent advances in aerodynamics inside the nsmb (navier-stokes multi-block) consortium. *AIAA paper*, 1998-0802, 1998.

[13] P.R. Spalart and S.R. Allmaras. A one equation turbulence model for aerodynamics flows. *AIAA paper*, 92-0439, 1992.

[14] M. Pascasio. Contribution expérimentale à l'étude de la couche limite se développant sur un profil d'aile en oscillation : phénomènes de transition et de décollement en écoulement instationnaire. Thèse de dotorat, Université de la Méditerranée (Aix-Marseille II), 1995.